Biochemistry & Analytical Biochemistry
ISSN: 2161-1009

Roy et al., Biochem Anal Biochem 2016, 5:2
DOI: 10.4172/2161-1009.1000278

Research Article Open Access

Report of Interaction Between Calf Thymus DNA and Pyrimidine-Annulated Spiro-Dihydrofuran

Swarup Roy[1*], Sintu Ganai[2], Raj Kumar Nandi[2], K.C. Majundar[2] and Tapan K. Das[1]

[1]Department of Biochemistry and Biophysics, University of Kalyani, West Bengal, India
[2]Department of Chemistry, University of Kalyani, West Bengal, India

Abstract

The study of binding interaction between pyrimidine-annulated spiro-dihydrofuran (PSDF) with calf thymus DNA (CTDNA) using UV absorption, fluorescence, circular dichroism (CD), and molecular docking methods. The experimental results revealed that PSDF preferred to bind to the groove of CTDNA with the binding constant (K) of 1.51×10^2 L/mol at 293 K. Based on the signs and magnitudes of the enthalpy change (ΔH = -33.25 kJ/mol) and entropy change (ΔS= -71.58 J/mol/K) in the binding process it can be concluded that the main interaction forces between PSDF and CTDNA in the binding process were van der Waals force and hydrogen bonding interaction. The results of CD experiments revealed that PSDF did not disturb native conformation of CTDNA and the significant binding of PSDF in PSDF-CTDNA complex was observed from the molecular docking results.

Keywords: PSDF; CTDNA; Interaction; Spectroscopy; Docking

Introduction

The interactions between DNA with various drug molecules act a prime role in the pharmaceutical sciences and drug design [1] as this kind of study provide insight into the mechanism of action of DNA-targeted drugs. The dominant binding class of small molecules with DNA can be classified as (i) covalent binding and (ii) non-covalent binding, including intercalative binding [2], nonspecific electrostatic interaction [3] and DNA major/minor groove binding [2]. Non-covalent binding is the predominant DNA-binding mode of the major two classes of small ligands [4–7].

Pyrimidine is constituents of nucleic acid and it shows diverse role in biological, pharmaceutical as well as agrochemical sectors. In recent times pyrimidine compounds have attracted enormous attention from researchers and are widely recognized as biologically useful systems because of their potential biological activities, such as antibacterial, antimicrobial, and anticancer, activities [8,9]. It is well established that furo [2, 3-*d*]-pyrimidine [10] derivatives have desirable pharmacological properties. The furo [2, 3-*d*]-pyrimidine derivatives act as antiulcer agents, muscle relaxants, antihistamines and diuretics [11]. As a result of the aforesaid medicinal activity, further biological testing's of pyrimidine derivatives remains a centre of attraction and it is essential to study the interaction of pyrimidine and DNA. As the reaction modes and binding properties during the interaction can help understand the functional mechanism of drugs, and provide theoretical basis for the development of new drugs targeted to DNA. So in this sense studying the interaction of DNA with pyrimidine derivatives is very important.

There are already several reports of interaction like Ramana et al. reported interaction of nelfinavir (NFV) with herring sperm DNA under physiological conditions [12]. Zhu et al. reported the interaction of 5-Hydroxymethyl-2-furfural (5-HMF) with calf thymus DNA [13]. Zhang et al. reported interaction of ferulic acid with calf thymus DNA [14]. Xie et al. reported Spectroscopic analyses on interaction of melamine, cyanuric acid and uric acid with DNA [15]. Hassan and Rauf reported multi-spectroscopic DNA binding study of 1,3,4-oxadiazole and 1,3,4-thiadiazole derivatives of fatty acid [16]. Silva et al. reported DNA binding of new copper (II) complexes with chalcone-derived thiosemicarbazones [17]. Recently Hassan and Rauf reported DNA binding study of 1,3,4-oxadiazole and 1,3,4-thiadiazole derivatives of fatty acid using multi-spectroscopic technique [16]. So, considering the medicinal as well as biological importance of pyrimidine it is noteworthy to study the interaction with DNA using well established spectroscopic and docking techniques.

In the present work in order to obtain the detailed information about the binding interaction between PSDF and CTDNA like the specific binding site, the binding modes, the binding constant and the interaction forces. The binding interaction of PSDF with DNA was investigated using UV–Vis absorption, fluorescence emission, circular dichroism spectroscopy, melting study and molecular docking. This study is expected to provide important insight into the interaction of Pyrimidine derivatives to DNA.

Experimental Procedures

Materials

The PSDF required for this study was prepared according to published procedure [18]. Synthesized PSDF (1 mM) was dissolved in methanol. Tris–base, and EDTA were purchased from Merck, Germany and ethidium bromide (EB) CTDNA were purchased from Sigma Chemicals, USA. Other molecular biology grade fine chemicals were purchased from SRL, India. All the other chemicals were of analytical reagent grade and double distilled water was used throughout.

Instrumentation

Fluorescence measurements were carried out on Agilent Technologies Cary-Eclipse fluorescence spectrophotometer well

***Corresponding author:** Swarup Roy, Department of Biochemistry and Biophysics, University of Kalyani, West Bengal, India Tel: (033) 25828750, 2582 8378 (Ext. 385), +91-9046546632; Fax: +91-33-25828282; E-mail: swaruproy2013@gmail.com, swaruproy@klyuniv.ac.in

Received: February 03, 2016; **Accepted:** May 31, 2016; **Published** June 03, 2016

Citation: Roy S, Ganai S, Nandi RK, Majundar KC, Das TK (2016) Report of Interaction Between Calf Thymus DNA and Pyrimidine-Annulated Spiro-Dihydrofuran. Biochem Anal Biochem 5: 278. doi:10.4172/2161-1009.1000278

equipped with attach Cary Temperature controller. The absorption spectra were recorded on a Cary 100 UV-Vis spectrophotometer, Agilent Technologies. Circular dichroic spectra were measured on a Jasco J-815 CD spectrometer.

Methods

UV-absorption spectra: The CTDNA solution was prepared by dissolving an appropriate amount of CTDNA in Tris-EDTA buffer (0.1 μM, pH 7.4) solution with stirring for 12 h at below 4°C. Absorption experiments were carried out keeping constant CTDNA concentration (50 μg/ml) whereby varying the PSDF concentration (4-24 μM). Spectral changes of CTDNA were monitored after adding different concentrations of PSDF by recording the UV-visible absorption in the range of 200-400 nm. All experiments were carried out in Tris-EDTA buffer (0.1 μM, pH 7.4) in a conventional quartz cell thermostatted for maintenance of the temperature.

Steady state fluorescence: At first, DNA (50 μg/ml) was added to aqueous EB solution (10 μg/ml) and maximum quantum yield for EB was achieved at 270 nm, so this wavelength has been selected as the excitation radiation for samples in the emission range of 550-700 nm. In the solution of EB and DNA different concentrations of PSDF (5-30 μM) were added successively at 293, 303, and 313 K.

Circular dichroism measurements: The concentration of CTDNA was kept constant (50 μg/ml) while varying the concentration of PSDF (0-10 μM) and the Tris-EDTA buffer was used as reference solution.

Thermal denaturation study: The absorbance of CTDNA (50 μg/ml) in TE buffer (0.1 μM, pH 7.4) was measured at 260 nm in a range from 40°C to 90°C. The study of thermal denaturation was performed in a spectrophotometer equipped with a Peltier temperature controller. CTDNA was taken in a cell and 10 μM of PSDF was added. Since analyzed profiles were almost linear in the melting region, melting temperature (T_m) was determined as the average of starting and final temperatures of the melting process.

Molecular docking: Docking operations were performed using version 4.0 of the AutoDock program package and the Lamarckian genetic algorithm (LGA) available in AutoDock 4.0, which was proven to be most reliable, successful and effective [19,20]. Structures of the compounds, PSDF were sketched by CHEMSKETCH (http://www.acdlabs.com) and convert it into PDB format from mol format by online OPENBABEL (http://www.vcclab.org/lab/babel/). The LGA was used in this docking study of the compounds PSDF with double-stranded DNA. The DNA duplex receptor structure from the Protein Data Bank (PDB ID 2dyw) contained 12 base pairs. The base pair sequence was CGCGAATTCGCG: GCGCTTAAGCGC. The compounds and DNA were added along with Gasteiger charges and polar hydrogen atoms using AutoDockTools version 1.5.2. AutoGrid was used to calculate the grid maps that represented the DNA in the docking process. Sufficiently large grids were chosen to include a significant part of the DNA. In all cases, we used grid maps with a grid box size of 106×110×102 points with a grid-point spacing of 0.375 Å. Then, we started the molecular docking via the LGA using default parameters. For PSDF ligand, ten independent docking runs were carried out. Visualization of the docked pose was done using Discovery digital studio molecular graphics programme.

Results and Discussion

UV-Vis spectra

From the Figure 1 it is clear that with addition of PSDF (4-24 μM) the intensity of peak of CTDNA at 260 nm constantly increases with slight blue shift and this indicates the possibility of interaction between PSDF and CTDNA. To determine the apparent association constant (K_{app}) Equation 1 is used as previously mentioned [21].

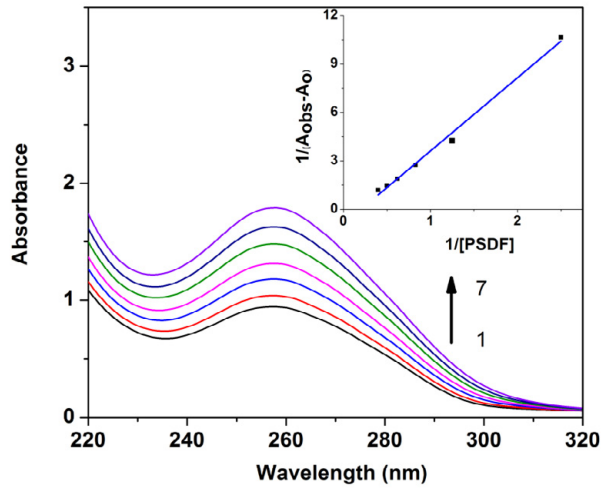

Figure 1: Absorption spectra of CTDNA in presence of PSDF (1-7): (4-24 μM), inset: Calculation of Kapp of CTDNA-PSDF complex.

$$\frac{1}{A_{obs}-A_0}=\frac{1}{A_C-A_0}+\frac{1}{K_{app}(A_C-A_0)[PSDF]} \quad (1)$$

Where, A_0 is the absorbance of CTDNA in the absence of PSDF and A_C is the recorded absorbance at 260 nm for CTDNA at different PSDF concentrations. The plot of $1/(A_{obs}-A_0)$ vs. 1/[PSDF] is linear and K_{app} estimated to be 2.00×10^4 L/mol (R= 0.9967, where R is the correlation coefficient) (Figure 1 inset) from the ratio of the intercept to the slope [21]. The low value of K_{app} clearly suggested formation of a weak complex between CTDNA and PSDF.

Fluorescence spectra

We have used ethidium bromide as a probe and fluorescence titration of solutions containing the DNA and EB with PSDF has been investigated. The molecular fluorophores EB, phenenthridine fluorescence dye forms soluble complexes with nucleic acids and emits intense fluorescence in the presence of DNA due to the intercalation of the planar phenenthridinium ring between adjacent base pairs on the double-helix [22,23]. The fluorescence emission spectra of intercalated EB with increasing concentrations of PSDF (5-30 μM) at 293, 303 and 313 K are shown in Figure 2. The result clearly shows the decrease of intensities of DNA-EB fluorescence in presence of PSDF.

The quenching properties can be explained by the following Stern-Volmer equation Equation 2 [24-27].

$$F_0/F=1+K_q\tau_0[Q]=1+K_{SV}[Q] \quad (2)$$

Where, F_0 and F are the fluorescence intensities in the absence and presence of a quencher, K_q is the bimolecular quenching rate constant, K_{SV} is the Stern Volmer constant, τ_0 is the average lifetime of the molecule in the absence of a quencher and [Q] is the concentration of the quencher. Since the fluorescence lifetime of a biopolymer is 10^{-8} s [24], the K_q value is calculated using the formula $K_q = K_{SV}/\tau_o$. In case of dynamic quenching the maximum scatter quenching collision constant

of various quenchers with the biopolymer is near 1×10^{10} L/mol/s [25]. Stern-Volmer plot of CTDNA-EB illustrates that the quenching of EB bound to DNA by PSDF is in good agreement with the linear Stern-Volmer equation (Equation 2), which proves that the partial replacement of EB from EB bound to DNA by nanoparticle results in a decrease in the fluorescence intensity. The low K_{SV} value (4.6×10^{-2} L/mol at 293 K) shows that PSDF can be bound loosely to the CTDNA molecule [24]. Details of the fluorimetric data are shown in Table 1 and the temperature dependent study indicating with rise in temperature the quenching constants increases.

Calculation of binding constant and binding site

From the fluorimetric data the binding constant (K) and number of binding site can be calculated using following Equation 3 [25-27].

$$log\frac{F_0-F}{F}=logK+n\log[Q] \quad (3)$$

Where, F_0 and F are the fluorescence intensities of the fluorophore in absence and in presence of different concentrations of PSDF [Q] respectively. A plot of log [(F_0–F)/F] vs. log [Q] gives a linear plot, whose slope equals to 'n' (the number of binding sites of PSDF on CTDNA) and the length of intercept on Y-axis equals to log K (Figure 3).

The values of K and n are shown in Table 2. The binding constant of PSDF with CTDNA was estimated to be $1.5.1\times10^{2}$ L/mol at 293 K. Ligands that are well-known groove binders show low values of binding constants in comparison with ligands that intercalate into DNA [28,29]. Thus in present study the fluorescence intercalators' displacements assay favors the groove-binding mode.

Thermodynamic parameters of DNA binding

The interactive forces like hydrophobic forces, electrostatic interactions, van der Waals interactions, hydrogen bonds, etc. may be involved in-between small molecule and biomolecules [30-34]. According to the data obtained for changes in enthalpy (ΔH) and entropy (ΔS), the mode of interaction between drug and biomolecules can be concluded as [35]: (1) ΔH > 0 and ΔS > 0, hydrophobic forces; (2) ΔH < 0 and ΔS < 0, van der Waals interactions and hydrogen bonds; (3) ΔH < 0 and ΔS > 0, electrostatic interactions [36]. When there is a little change of temperature, the change of ΔH remains unchanged, and thereby its value and that of ΔS can be determined from the following Van't Hoff equation (Equation 4).

$$\ln K=-\Delta H/RT+\Delta S/R \quad (4)$$

Where, K is the binding constant at the corresponding temperature and R is gas constant. The values of ΔH and ΔS were obtained from the slope and intercept of the linear plot (Equation 4) based on lnK vs. 1/T (Figure 4).

The free energy change (ΔG) was estimated using (Equation 5).

$$\Delta G=\Delta H-T\Delta S=-RT\ln K \quad (5)$$

The values of ΔH, ΔS and ΔG for the interaction between PSDF and DNA are listed in Table 3.

An experimental negative value of ΔG revealed that the interaction process is spontaneous, while the negative ΔH and ΔS values indicated that the interaction is driven by van der Waals interactions and hydrogen bonds interactions. According to the thermodynamic data, the formation of the CTDNA-PSDF complex is in favor of enthalpy, free energy for the formation of the aforesaid complex.

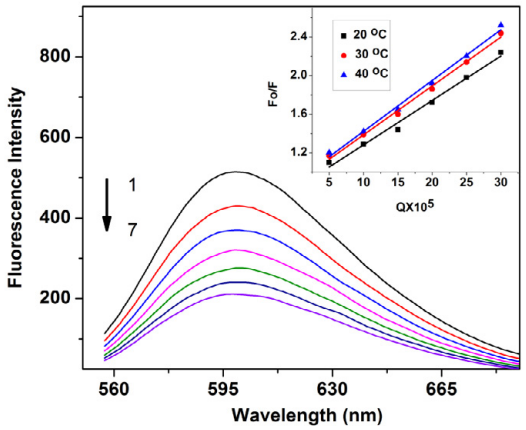

Figure 2: Fluorescence quenching spectra of CTDNA in presence of PSDF (5-30 μM), inset: S-V plot for PSDF and CTDNA at 293, 303, and 313 K respectively.

T(°C)	R[a]	K_{SV} (L/mol) ×10^{-2}	K_q (L/mol/S)×10^6
20	0.9948	4.6	4.6
30	0.9974	5.06	5.06
40	0.9975	5.26	5.26
[a] correlation coefficient			

Table 1: The Stern–Volmer constants and quenching constants of CTDNA by PSDF.

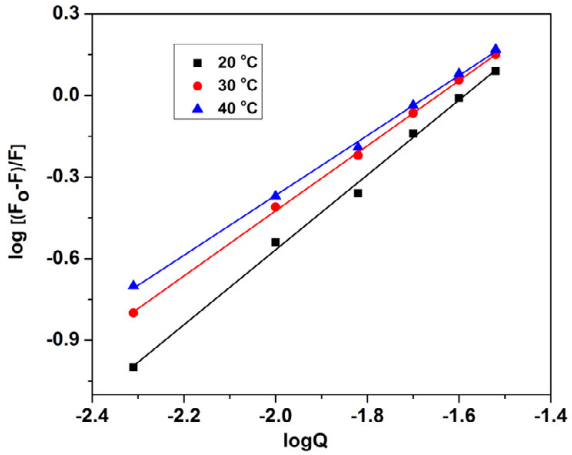

Figure 3: Plots of the PSDF quenching effect on CTDNA-EB fluorescence at 293, 303, and 313 K respectively.

Circular dichroism spectroscopy

CD spectra of CTDNA incubated in presence of PSDF (5 μM) were recorded. The observed CD spectrum of DNA consists of a positive band at 275 nm due to base stacking and a negative band at 245 nm due to helicity, which are characteristics of DNA in the right handed B form. When PSDF was incubated with DNA, the CD spectra exhibited slight changes mainly in the positive bands (Figure 5).

It is reported that, in case of minor groove binding and electrostatic binding, the CD spectra show insignificant change whereas, intercalating binding causes a remarkable change in the positive and negative bands [37]. As illustrated in Figure 5, after addition of PSDF

T(°C)	R[a]	K (L/mol)×10²	n
20	0.9983	1.51	1.38
30	0.9997	0.93	1.20
40	0.9993	0.67	1.10
[a] correlation coefficient			

Table 2: Binding constants (K) and number of binding sites (n) on CTDNA for PSDF.

T(°C)\	R[a]	ΔH (kJ/mol)	ΔS (J/mol/K)	ΔG (kJ/mol)
20	0.9974	-33.25	-71.58	-12.27
30	-	-33.25	-71.58	-11.56
40	-	-33.25	-71.58	-10.84

Table 3: Thermodynamic parameters for the binding of the PSDF to CTDNA at different temperature.

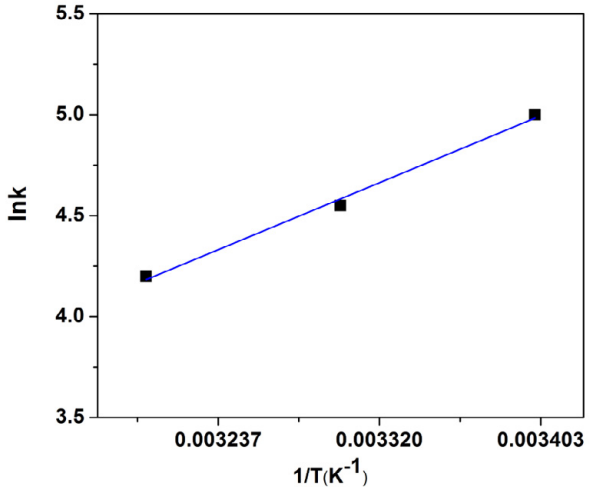

Figure 4: The Vant Hoff's plot for the interaction of CTDNA and PSDF.

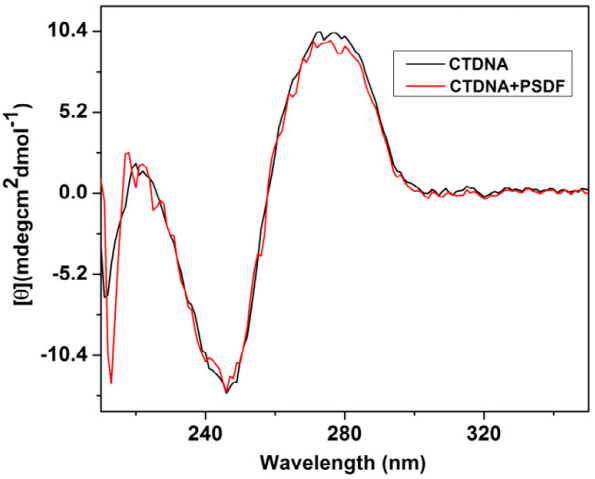

Figure 5: CD spectra of CTDNA-PSDF system, CTDNA (50 μg/ml) and PSDF (5 μM).

to the DNA solution does not produced any significant change in the intrinsic CD spectrum of the DNA indicating that binding of PSDF with CTDNA does not disturb the stacking of bases. This observation rules out intercalative binding and thereby indicates that PSDF may bind to the DNA though groove binding.

Melting studies

Thermal behaviours of DNA in the presence of PSDF can give the information about the DNA conformational changes when the temperature is raised, and it can also predict about the strength of interactive forces existing between PSDF and DNA. According to the literature, [38,39] the intercalation of natural or synthesized organic and metallo-intercalators generally results due to considerable increase in melting temperature.

The melting curves of CTDNA in absence and presence of the PSDF are presented in Figure 6. Here, the thermal denaturation experiment carried out for DNA in absence of PSDF revealed a T_m value of 68 (± 0.2°C) under the experimental conditions, whereas the observed melting temperature of DNA in presence of PSDF in turn slightly increased to (T_m) 71 (± 0.2°C). Addition of PSDF to DNA resulted in a small increase in melting temperature by 3 ± 0.2°C. So, melting studies revealed that binding of PSDF to CTDNA resulted in a small increase in melting temperature, which is unlikely in case of classical intercalators; rather, it indicates external binding. Small change in melting temperature has also been observed in case of an unusual mode of binding through partial intercalation [40]. The present study reveals that upon binding with PSDF the T_m of CTDNA is increased by 3°C supports the possibility of groove binding mode.

Molecular docking

In an effort to interpret the molecular interactions of PSDF with DNA, molecular docking was performed to simulate the interactions between the aforesaid molecules. Molecular docking technique is an attractive scaffold to understand the Drug–DNA interactions for the rational drug design and discovery, as well as in the mechanistic study by placing a small molecule into the binding site of the target specific region of the DNA mainly in a non-covalent fashion [41,42].

It is well known that the interactions of chemical species with the minor groove of B-DNA differ from those occurring in the major groove, both in terms of electrostatic potential and steric effects, because of the narrow shape of the former. In contrast to the major groove, small molecules preferentially interact with the minor groove due to little steric interference. Figure 7 shows the pictorial diagram of docking between PSDF and choose B-DNA and the resulting binding

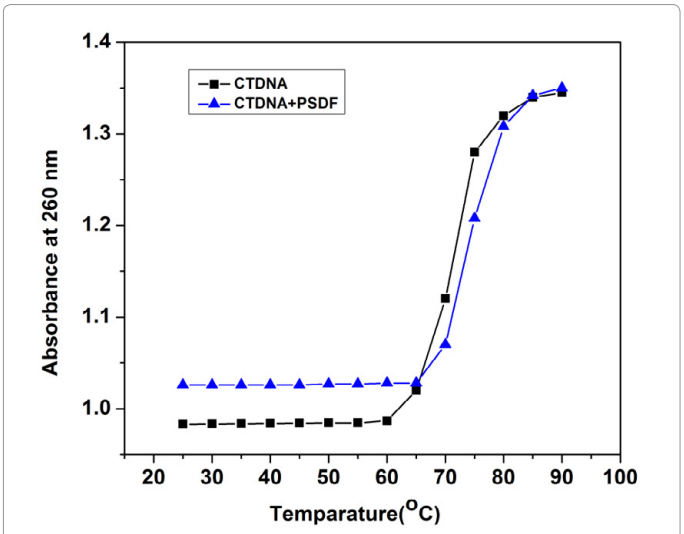

Figure 6: Melting temperature study for CTDNA-PSDF interaction.

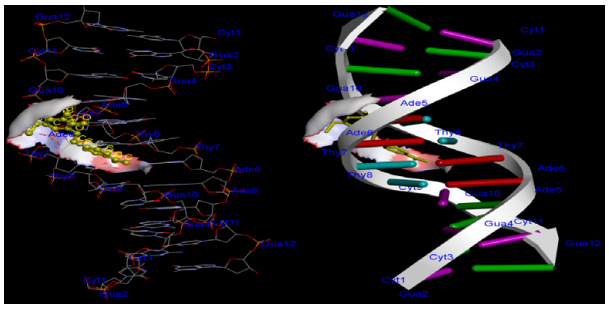

Figure 7: Docking of interaction between PSDF to CTDNA.

energy of docked compounds PSDF was found to be −8.89 kcal/mol and the results indicative of strong and spontaneous binding and the picture also indicative of groove binding rather intercalation mode.

Conclusion

From the above results it can be concluded that binding of PSDF to CTDNA occurs and here PSDF may acts as a groove-binder as evident from the spectroscopic, DNA melting and docking experiments.

Acknowledgement

Swarup Roy thanks Department of Science and Technology (New Delhi, India) for a DST INSPIRE fellowship (IF 110421).

References

1. Yang ZS, Zhang DP, Long HY, Liu YC (2008) Electrochemical behavior of gallic acid interaction with DNA and detection of damage to DNA. Electro anal Chem 624: 91-96.
2. Erkkila KE, Odom DT, Barton JK (1999) Recognition and reaction of metallointercalators with DNA. Chem Rev 99: 2777-2796.
3. Carter MT, Rodriguez M, Bard AJ (1989) Voltammetric studies of the interaction of metal chelates with DNA 2-Tris-chelated complexes of cobalt (III) and iron (II) with 1,10-phenanthroline and 2,2'-bipyridine. Jour Am Chem Soc 111: 8901-8911.
4. Bischoff G, Hoffmann S (2002) DNA-binding of drugs used in medicinal therapies. Curr Med Chem 9: 312-348.
5. Han X, Gao X (2001) Sequence specific recognition of ligand-DNA complexes studied by NMR. Curr Med Chem 8: 551-581.
6. Neidle S, Nunn CM (1998) Crystal structures of nucleic acids and their drug complexes. Nat Prod Rep 15: 1-15.
7. Rohs R, Bloch I, Sklenar H, Shakked Z (2005) Molecular flexibility in *ab initio* drug docking to DNA: binding-site and binding-mode transitions in all-atom Monte Carlo simulations. Nucleic Acids Res 33: 7048-7057.
8. Li X, Zheng A, Liu B, Yu X, Yi P (2010) Synthesis of [1,2,4] Oxadiazolo [4,5-a] thiazolo [2,3-b] pyrimidin-9(10H)-ones via 1,3-Dipolar Cycloaddition of Nitrile Oxide to Thiazolo [3,2-a]pyrimidin-3-one Derivatives. Chin J Chem 28: 977–980.
9. Abd El-Galil EA, Maigali SS, Abdulla MM (2008) Synthesis, and analgesic and anti-parkinsonian activities of thiopyrimidine, pyrane, pyrazoline, and thiazolopyrimidine derivatives from 2-chloro-6-ethoxy-4-acetylpyridine. Monatsh Chem 139: 1409–1415.
10. De Clercq E (2003) Highly potent and selective inhibition of varicella-zoster virus replication by bicyclic furo [2,3-d] pyrimidine nucleoside analogues. Med Res Rev 23: 253-274.
11. Melik-Ogandzhanyan RG, Khachatryanand VE, Gapoyan AS (1985) Furo-, Thieno-, and Pyrrolo-[2,3-d] pyrimidines. Russ Chem Rev 54: 262-276.
12. Ramana MMV, Betkar R, Nimkar A, Ranade P, Mundhe B, et al. (2015) In vitro DNA binding studies of antiretroviral drug nelfinavir using ethidium bromide as fluorescence probe. J Photochem Photobiol B 151: 194-200.
13. Zhu J, Chen L, Dong Y, Li J, Liu X (2014) Spectroscopic and molecular modeling methods to investigate the interaction between 5-Hydroxymethyl-2-furfural and calf thymus DNA using ethidium bromide as a probe. Spectrochim Acta A Mol Biomol Spectrosc 124: 78-83.
14. Zhang S, Sun X, Qu F, Kong R (2013) Molecular spectroscopic studies on the interaction of ferulic acid with calf thymus DNA. Spectrochim Acta A Mol Biomol Spectrosc 112: 78-83.
15. Xie J, Chen D, Wu Q, Wang J, Qiao H (2015) Spectroscopic analyses on interaction of melamine, cyanuric acid and uric acid with DNA. Spectrochim Acta A Mol Biomol Spectrosc 149: 714-721.
16. Hassan MF, Rauf A (2016) Synthesis and multi-spectroscopic DNA binding study of 1,3,4-oxadiazole and 1,3,4-thiadiazole derivatives of fatty acid. Spectrochim Acta A Mol Biomol Spectrosc 153: 510-516.
17. Da Silva JG, Despaigne AAR, Louro SRW, Bandeira CC, Souza-Fagundes EM, et al. (2013) Cytotoxic activity, albumin and DNA binding of new copper (II) complexes with chalcone-derived thiosemicarbazones. Eur J Med Chem 65: 415-426.
18. Majumdar KC, Ganai S, Nandi RK (2011) Regioselective synthesis of pyrimidine-annulated spiro-dihydrofurans by silver-catalyzed 5-endo-digcyclization. New J. Chem 35: 1355–1359.
19. Mandal A, Ghosh S, Bothra AK, Nanda AK, Ghosh P (2012) Synthesis of friedelan triterpenoid analogs with DNA topoisomerase IÎ± inhibitory activity and their molecular docking studies. Eur J Med Chem 54: 137-143.
20. Marinelli L, Lavecchia A, Gottschalk KE, Novellino E, Kessler H (2003) Docking studies on alphavbeta3 integrin ligands: pharmacophore refinement and implications for drug design. J Med Chem 46: 4393-4404.
21. Stephanos JJ (1996) Drug-protein interactions: two-site binding of heterocyclic ligands to a monomeric hemoglobin. J Inorg Biochem 62: 155-169.
22. Butour JL, Macquet JP (1977) Differentiation of DNA-platinum complexes by fluorescence. The use of an intercalating dye as a probe. Eur J Biochem 78: 455-463.
23. Geall AJ, Blagbrough IS (2000) Rapid and sensitive ethidium bromide fluorescence quenching assay of polyamine conjugate–DNA interactions for the analysis of lipoplex formation in gene therapy. J Pharm Biomed Anal 22: 849-859.
24. Psomas G, Tarushi A, Efthimiadou EK (2008) Synthesis, characterization and DNA-binding of the mononuclear dioxouranium (VI) complex with ciprofloxacin. Polyhedron 27: 133-138.
25. Jiang M, Xie MX, Zheng D, Liu Y, Li XY, et al. (2004) Spectroscopic studies on the interaction of cinnamic acid and its hydroxyl derivatives with human serum albumin. J. Mol. Struct 692: 71–80.
26. Roy S, Das TK (2014) Spectroscopic studies of interaction between biologically synthesized silver nanoparticles and bovine serum albumin. J Nanosci Nanotechnol. 14: 4899-4905.
27. Roy S, Das TK (2015) Study of interaction between tryptophan, tyrosine, and phenylalanine separately with silver nanoparticles by fluorescence quenching method. J Appl Spectrosc 82: 598-606.
28. Boger DL, Fink BE, Hedrick MP (2000) Total synthesis of distamycin a and 2640 analogues: a solution-phase combinatorial approach to the discovery of new, bioactive DNA binding agents and development of a rapid, high-throughput screen for determining relative DNA binding affinity or DNA binding sequence selectivity. J Am Chem Soc 122: 6382–6394.
29. Lee M, Rhodes AL, Wyatt MD, Forror S, Hartley JA (1993) GC base sequence recognition by oligoimidazolecarboxamide and C-terminus-modified analogs of distamycin deduced from circular dichroism, proton nuclear magnetic resonance, and methidium propyl ethylenediamine tetraacetate-iron (II) foot printing studies. Biochemistry 32: 4237–4245.
30. Ross PD, Subramanian S (1981) Thermodynamics of protein association reactions: forces contributing to stability. Biochemistry 20: 3096-3102.
31. Roy S, Das TK (2014) Investigation of interaction between casein enzyme hydrolysate and biosynthesized silver nanoparticles by spectroscopy. Nanosci Nanotechnol Lett 6: 547-554.
32. Roy S, Sadhukhan R, Ghosh U, Das TK (2015) Interaction studies between biosynthesized silver nanoparticle with calf thymus DNA and cytotoxicity of

silver nanoparticles. Spectrochim Acta A 141: 176-184.

33. Roy S, Das TK (2015) The interaction of biosynthesized gold nanoparticles with casein enzyme hydrolysate. Journal of Bionanoscience 9: 424-430.

34. Roy S, Das TK (2016) Interaction of biosynthesized gold nanoparticles with BSA and CTDNA: A multi-spectroscopic approach (In Press).

35. Nike DB, Moorty PN, Priyadarsini KI (1990) Non-radiative energy transfer from 7-amino coumarin dyes to thiazine dyes in methanolic solutions. Chem Phys Lett 168: 533–538.

36. Shahabadi N, Fatahi A (2010) Multispectroscopic DNA-binding studies of a tris-chelate nickel (II) complex containing 4,7-diphenyl 1,10-phenanthroline ligands. J Mol Struct 970: 90–95.

37. Sahoo D, Bhattacharya P, Chakravorti S (2010) Quest for mode of binding of 2-(4-(dimethylamino) styryl)-1-methylpyridinium iodide with calf thymus DNA. J Phys Chem B 114: 2044-2050.

38. Jain SS, Polak M, Hud NV (2003) Controlling nucleic acid secondary structure by intercalation: Effects of DNA strand length on coralyne-driven duplex disproportionation. Nucleic Acids Res 31: 4608-4615.

39. Mergny JL, Duval-Valentin G, Nguyen CH, Perrouault L, Faucon B, et al. (1992) Triple helix-specific ligands. Science 256: 1681-1684.

40. Rajendran A, Nair BU (2006) Unprecedented dual binding behaviour of acridine group of dye: A combined experimental and theoretical investigation for the development of anticancer chemotherapeutic agents. Biochim Biophys Acta 1760: 1794–1801.

41. Shahabadi N, Fili SM, Kheirdoosh F (2013) Study on the interaction of the drug mesalamine with calf thymus DNA using molecular docking and spectroscopic techniques. J Photochem Photobiol B 128: 20-26.

42. Caruso F, Rossi M, Benson A, Opazo C, Freedman D et al. (2012) Ruthenium-arene complexes of curcumin: X-ray and density functional theory structure, synthesis, and spectroscopic characterization, in vitro antitumor activity, and DNA docking studies of (p-cymene)Ru (curcuminato) chloro. J Med Chem 55: 1072-1081.